JOURNAL OF CATALYSIS **136**, 126–140 (1992)

Preparation and Characterization of Chlorine-Free Ruthenium Catalysts and the Promoter Effect in Ammonia Synthesis

3. A Magnesia-Supported Ruthenium Catalyst

KEN-ICHI AIKA,[1] TOMIKO TAKANO, AND SHUZO MURATA

Department of Environmental Chemistry and Engineering, The Graduate School at Nagatsuta, Tokyo Institute of Technology, 4259 Nagatsuta, Midori-ku, Yokohama 227, Japan

Received September 17, 1991; revised February 7, 1992

The support and promoter effects of Ru in ammonia synthesis were studied systematically using Ru carbonyl, $Ru_3(CO)_{12}$, as a precursor of the Ru catalyst. MgO was found to be the most effective support among several pure oxides. This high activity is thought to be due to the high Ru dispersion, the Cl-free system, and the basicity of the support. Modifying MgO by adding other oxides was also tried. Na_2O–MgO and Al_2O_3–MgO supports were found to be as effective as the pure MgO. Fourteen kinds of metal nitrates, including alkali metals, alkali earth metals, and lanthanides, were tested as promoters of Ru/MgO prepared from $Ru_3(CO)_{12}$. Alkali metal nitrates (Cs^+, Rb^+, and K^+), especially $CsNO_3$, were most effective. The synthesis rate was greatest when the Cs/Ru ratio was as low as 1.0, where the activity was 20 times as high as that without $CsNO_3$ at 588 K and under 80 kPa of $N_2 + 3H_2$. $CsNO_3$ was considered to be disproportionated to CsOH during the hydrogen treatment. The alkali promoter proved to act not only as a Cl scavenger in the case of a Cl-containing Ru catalyst but also as an electronic surface modifier to Ru. Hydrogen chemisorption studies disclosed that alkali covered mostly the Ru surface but had a weak interaction with the MgO surface. The importance of surface morphology in the combination of Ru and promoter was noted. Ru–CsOH/MgO (5 wt%; Cs/Ru = 1) was even more active than 4.7 wt% Ru–K/AC and was comparable to the Raney Ru–$CsNO_3$ catalyst, which had previously been reported to be the most active catalyst at 573 K and under 80 kPa of $N_2 + 3H_2$.

INTRODUCTION

Ruthenium has been reported to be quite sensitive as a support and a promoter in ammonia synthesis (*1*). $RuCl_3$ has been used as a precursor because it is a stable and common compound (*2–4*). In the previous work in this series, we pointed out that chlorine left on Ru/MgO retarded ammonia synthesis and that alkali could remove it (*5*). We have now tested the various Cl-free Ru precursors in attempts to prepare more effective catalysts. We previously found $Ru_3(CO)_{12}$ and $Ru(NO)(NO_3)_3$ to be effective precursors among four compounds, including $Ru(acac)_3$ and K_2RuO_4, when they were supported on Al_2O_3 (*6*). The alkali promoters promoted the activity not only by neutralizing Cl but also by affecting the Ru surface electronically; this was examined using the Cl-free $Ru_3(CO)_{12}/Al_2O_3$ catalysts (*6*).

When $RuCl_3$ was used as a precursor, the support and promoter effect was complicated because of the remaining chlorine. A Cl-free system led us to find new promoters, lanthanide nitrates (*7*), which were effective when applied to Cl-free $Ru_3(CO)_{12}/Al_2O_3$ catalyst. The promoter action of the lanthanides has been discussed especially with respect to surface chemistry and morphology (*7*). We have again tried to study systematically the support and promoter effect using Cl-free $Ru_3(CO)_{12}$ precursor. Because a promoter can interact with both Ru and a support, it is important to control the promoter to interact exclusively with Ru.

In the case of supported (2 wt%) ruthenium catalyst, the activity per gram ranges

---

[1] To whom correspondence should be addressed.

0021-9517/92 $5.00

over 3 orders of magnitude, as shown in the previous work (*3*) or in Fig. 14. On the other hand, ruthenium dispersion (H/Ru) ranges about 1 order of magnitude depending on the supports and promoters (*2, 3, 6*). Thus, the chemical effect of support and promoter is more important than the physical factor. In this work, first we tested several simple oxides as supports without a promoter. Here, the activity was compared mainly on the basis of catalyst weight for convenience. Because MgO was the most effective support, we tested supports with two components, one of which was MgO. Then we tested 14 kinds of metal nitrates, including alkali metals, alkali earth metals, and lanthanides, as promoters of a Ru/MgO catalyst prepared from $Ru_3(CO)_{12}$. Here, the activities were also compared on a weight basis. Finally, we made a detailed study of the active catalysts Ru–CsOH/MgO and Ru–BaO/MgO, where the activities were compared on the basis of TOF in addition to weight.

METHODS

A support that had been baked at 773 K for 6 h (and some at 873 K for 3 h) was impregnated with $Ru_3(CO)_{12}$ (Aldrich) in tetrahydrofurane (THF) solution (orange). The amount of Ru loadings was usually 2 wt%. The $Ru_3(CO)_{12}$–THF–support system, stirred for 4 h (yellow), was evacuated in the rotary evaporator, dried, pressed, and crashed to 10-mesh size (white). $Ru_3(CO)_{12}$ was transferred to the support almost completely. No orange powder of $Ru_3(CO)_{12}$ was observed on the wall of the rotary evaporator after the impregnation. It was subsequently moved into a reactor, evacuated at 623 K for 2 h to eliminate CO (gray), and finally reduced with hydrogen at 673 or 873 K (gray). Evaporation and condensation of $Ru_3(CO)_{12}$ was not observed at the upper part of the reactor. However, when the catalyst (Ru/MgO) was baked in air at 623 K rather than decarbonylated *in vacuo*, the sample gave no activity even when later reduced at 673 K, probably due to the evaporation of $Ru_3(CO)_{12}$.

We baked the following pure oxides at 773 K for 6 h and used them as promoters: γ-Al_2O_3 (the reference catalyst of the Catalysis Society of Japan, JRC-ALO-4), MgO (two lots from Soekawa Chemical and one lot from Kanto Chemical), TiO_2 (MCB), Nb_2O_5 (Mitsui Metal), and CaO (as $CaCO_3$, Soekawa Chemical). We prepared alkali-doped MgO by impregnating MgO with an alkali nitrate (6 h) in aqueous solution and baking it at 773 K for 6 h. We obtained $LiNO_3$, $NaNO_3$, and KNO_3 (special grade) from Kanto and $RbNO_3$ (99%) and $CsNO_3$ (99%) from Mitsuwa Chemical and Soekawa, respectively. Al_2O_3–MgO mixed oxide was prepared by coprecipitating $Al(NO_3)_3$ (Wako Pure Chemical) and $Mg(NO_3)_2$ (Kanto) in aqueous solutions of ammonia or urea and by baking at 773 K for 6 h.

Fourteen kinds of promoter were added to Ru/MgO, decarbonylated from $Ru_3(CO)_{12}$/MgO. After evacuating $Ru_3(CO)_{12}$/MgO at 723 K for 2 h, we impregnated 1 g of the sample with aqueous metal nitrate solution. Alkali nitrates were obtained from the source noted previously; $Ca(NO_3)_2 \cdot 4H_2O$, $Sr(NO_3)_2$, $Ba(NO_3)_2$, $La(NO_3)_3 \cdot 6H_2O$, $AgNO_3$, and $Ce(NO_3)_3 \cdot 6H_2O$ came from Kanto; $Pr(NO_3)_3 \cdot 6H_2O$, $Nd(NO_3)_3 \cdot 6H_2O$, $Sm(NO_3)_3 \cdot 6H_2O$, $Gd(NO_3)_3 \cdot 6H_2O$, and $Dy(NO_3)_3 \cdot 5H_2O$ were purchased from Mitsuwa. After standing for several hours, a sample was dried at 373 K and reduced with hydrogen, usually at 623 K, in a reactor. The ratio of alkali metal to ruthenium metal was usually 1 : 1. We prepared Ru/MgO and Ru/Al_2O_3 from $RuCl_3$ as reference catalysts (*5, 6*).

We used both a conventional flow system (101 kPa) (*5, 8*) and a closed circulation system (80 kPa) to measure the rate of ammonia synthesis below 673 K. $N_2 + 3H_2$ gas (60 ml/min), deoxidized through Pd/Al_2O_3 and active carbon trap at 195 K, was used for the ammonia synthesis. Hydrogen was passed for the reduction of the catalyst at a rate of 60 ml/min. In flowing hydrogen, temperature was increased for 1.5 h to the programmed treatment temperature and stood at that temperature for 4 h. The rate of ammonia synthesis was determined by the decrease rate of electron conductivity of diluted sulfuric acid solution, which fixed the produced ammonia under the flow system (*5, 8*), and it was measured by a volume decrease of gases in the closed circulation system where produced ammonia was fixed in a liquid N_2 trap (*2, 3*).

After the catalyst was treated with hydrogen at 673 K for 2 h and evacuated at 673 K for 1 h, we measured the hydrogen chemisorption at 273 K in a closed circulation system. We treated a sample with alkali promoter at 623 K and calculated the amount of hydrogen adsorption by extrapolating a liner portion of an adsorption isotherm measured above 20 Torr to zero pressure. BET area was measured using nitrogen.

We measured the XPS spectra of each catalyst with an ESCA-750 spectrometer (Shimadzu). Catalysts were treated with hydrogen at each temperature for 4 h and kept from the air to obtain the spectra. We used impurities of C 1*s* (284.6 eV) and Au $4f_{7/2}$ (83.8 eV) as the standard values for determining the binding energies and calculated the concentration of elements on the basis of cross section data reported.

The state of Ru catalyst during the decomposition of $Ru_3(CO)_{12}$ and the reduction was studied by EXAFS at LB-10 of the Laboratory of High Energy Physics in Tsukuba. We evacuated the 20-mm-diameter pressed sample and treated it with hydrogen in a thin glass reactor for EXAFS study.

RESULTS

Support Effect on Cl-Free Ru Catalyst: Single Component Oxides

We impregnated typical oxides, MgO, CaO, TiO_2, Nb_2O_5, and Al_2O_3, measured with $Ru_3(CO)_{12}$ to prepare supported Ru catalysts and the rates of ammonia synthesis on these catalysts. The results appear in Table 1. The activity seems to correlate roughly with the basicity of the support. MgO was the most effective support. We noted an induction period of about 24 h before there was a constant production of ammonia on Ru/CaO. CaO was obtained by baking $CaCO_3$. Surface carbonate that has not been completely eliminated is thought to react with hydrogen over the Ru surface, and this might inhibit the ammonia synthesis reaction on Ru/CaO. Sometimes, also, a short induction period (0 to 1 h) was seen for Ru/MgO, probably due to the same reaction.

TABLE 1

Support and Ru Precursor Effects in Ammonia Synthesis over 2 wt% Ru Catalyst[a] under 80 kPa of $N_2 + 3H_2$

Support	Rate (μmol NH_3 h^{-1} g^{-1})		H/Ru
	673 K	623 K	
MgO^b	379	174	0.68
MgO^c	364	—	—
MgO^d	—	184	0.45
MgO^e	—	20	0.06
MgO^f	—	44	0.18
CaO^g	176	—	—
Al_2O_3	62	—	—
TiO_2	5	—	—
Nb_2O_5	7	—	—

[a] Supports were heated at 773 K and impregnated with $Ru_3(CO)_{12}$. All catalysts were treated with hydrogen at 673 K for 4 h before reaction.

[b] Obtained from Soekawa Ltd.; surface area of 16 m^2 g^{-1} (90 m^2 g^{-1} for other MgO^{c-f}).

[c] Sample without evacuation.

[d] Treated in H_2 at 673 K.

[e] $RuCl_3$ is a precursor, treated in H_2 at 723 K.

[f] $RuCl_3$ is a precursor, treated in H_2 at 923 K.

[g] $CaCO_3$ is a precursor.

We compared Ru/MgO and Ru/Al_2O_3 prepared from $Ru_3(CO)_{12}$ with those prepared from $RuCl_3$. The results appear in Table 1 and Fig. 1. $RuCl_3$ precursor gave less activity, probably because of chlorine left after reduction at 723 K (*5, 6*). We also compared the activities according to reduction temperature. The activity and the Ru dispersion (H/Ru) of the catalyst prepared from $RuCl_3$ increased as reduction temperature increased, up to 923 K (Table 1, Fig. 1), likely

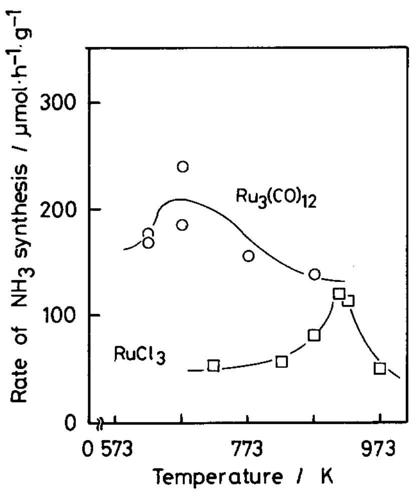

FIG. 1. Ammonia synthesis rate at 673 K under 101 kPa N_2 + $3H_2$ over 2 wt% Ru/MgO with different Ru precursors ($Ru_3(CO)_{12}$ and $RuCl_3$) correlated with hydrogen treatment temperature.

due to chlorine elimination. However, the activity is still low when compared with that of $Ru_3(CO)_{12}$/MgO because of sintering at the higher temperature (*5*). Conversely, Ru/MgO prepared from $Ru_3(CO)_{12}$ showed high activity when treated at 673 K. The activity increased slightly from 174 to 184 when treated at higher temperatures (623 to 673 K), but Ru dispersion (H/Ru) decreased from 0.68 to 0.45. The low activity of the catalyst reduced at 623 K might reflect the incomplete desorption of surface OH on MgO, because the reduction was complete at this temperature, as shown by EXAFS data. The activity decreased at higher temperatures probably because of the sintering.

Figure 2 presents the EXAFS spectra of catalysts and reference compounds. Vibrational structure $X(k)$ for the Ru K-edge X-ray spectrum is multiplied by k^3, where k is a photon wave number, and the $k^3X(k)$ value is shown as a function of bond distance between the Ru atom and the surrounding atom (*9*). The spectrum of $Ru_3(CO)_{12}$/MgO (a) resembles that of $Ru_3(CO)_{12}$ (A). Six CO molecules of $Ru_3(CO)_{12}$ may have been replaced with three surface oxygen atoms on MgO: $((CO)_2RuO)_3$/MgO (*9*, *10*). The spectrum after evacuation at 623 K (b) seems to resemble the mixture of that of Ru metal cluster (C) and that of RuO_2 (B), although the latter is a minor component of (b). Ru atoms make a metal cluster after decarbonylation *in vacuo* at 623 K, but it is partly oxidized (due to contamination of air during EXAFS measurement). Reduced samples, Ru/MgO (c) and Ru–CsOH/MgO (d), show spectra resembling the Ru metal cluster, Raney Ru (C). We observed no peaks suggesting the Ru–CsOH interaction (d). Even if Ru-promoter bonding occurred, EXAFS spectra might not reflect the surface change because of a low CsOH concentration on the Ru surface.

Support Effect on Cl-Free Ru Catalyst: Modification of MgO

To increase the basicity, we mixed the most effective support oxide, MgO, with another oxide. The oxide of the second element is acknowledged here as a part of the support because it is added to MgO and calcined before the $Ru_3(CO)_{12}$ is impregnated. Adding a small amount of alkali metal oxide

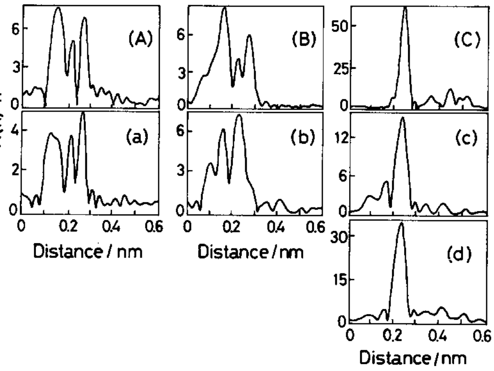

FIG. 2. Magnitudes of the k^3-weighted Fourier transformation of the EXAFS spectra of $Ru_3(CO)_{12}$/MgO catalysts and reference compounds. The spectra are the data for the extended structure beyond the K-adsorption edge of ruthenium. (a) $Ru_3(CO)_{12}$/MgO sample before evacuation; (A) $Ru_3(CO)_{12}$ for reference; (b) $Ru_3(CO)_{12}$/MgO sample after evacuation at 623 K; (B) RuO_2 for reference; (c) Ru/MgO after reduction at 623 K; (d) Ru–CsOH/MgO (Cs^+/Ru = 1/1) after reduction at 623 K; and (C) Raney Ru for reference.

TABLE 2

Effect of Addition to MgO in Ammonia Synthesis under 101 kPa of $N_2 + 3H_2$ over 2 wt% Ru/Alkali Metal Oxide–MgO[a]

Support	Alkali (mol%)	Rate (μmol NH_3 h^{-1} g^{-1})		E_a (kcal mol^{-1})
		673 K	623 K	
MgO		379	170	28.5
Li_2O–MgO	0.2	342	120	25.0
Na_2O–MgO	0.2	348	123	—
K_2O–MgO	0.2	419	154	27.9
Rb_2O–MgO	0.2	442	192	25.8
Cs_2O–MgO	0.2	436	186	28.2
Na_2O–MgO	1.0	458	204	25.7

[a] $Ru_3(CO)_{12}$ was impregnated after alkali metal nitrate–MgO supports were calcined in air at 773 K for 6 h. All catalysts were treated with hydrogen at 673 K for 4 h; 0.2 mol% alkali metal oxide (M_2O)–MgO corresponds to M/Ru = 0.25 (mol ratio).

to MgO increases both basicity and surface area (*11, 12*). The activity of 2 wt% Ru supported on MgO doped with 0.2 mol% of alkali is shown in Table 2. Only 0.2 mol% of Rb^+ and Cs^+ and 1.0 mol% of Na^+ increased the activity to some degree. However, the promotion was less remarkable than that of the alkali "promoter," which is described later.

Al_2O_3 is reported to increase the basicity of MgO up to six times (*13*). We mixed 10 mol% of Al^{3+} with Mg^{2+} by precipitating it with ammonia or urea. The results are not good (Table 3). The values are lower than those on 2 wt% Ru/MgO. Interestingly the apparent activation energies (19 kcal mol^{-1}) are midway between those on Ru/MgO (28 kcal mol^{-1}) and those on Ru/Al_2O_3 (13 kcal mol^{-1}) (*7*).

Addition of Promoter Nitrates to Chlorine-Free Ru/MgO

Ru/MgO, prepared from $Ru_3(CO)_{12}$ and proved to be most effective without a promoter, was impregnated with various nitrates. The promoters were thought to undergo disproportionation during hydrogen treatment and finally to become oxides and/or hydroxides (*2*). The promoter elements are classified into three categories: alkali metals, alkali earth metals, and lanthanides.

The activities of 2 wt% Ru/MgO promoted with various alkali metal nitrates (M/Ru = 1/1 mol ratio) are shown as a function of reciprocal temperature in Fig. 3. Roughly speaking, the effectiveness of the promoter is inversely related to the electronegativities of "compounds" (CsOH < RbOH = KOH < NaOH), as has been reported previously for Cl^--containing Ru catalysts (*2, 3*). In Fig. 3, the activity is greatest where ammonia partial pressure reaches the equilibrium value. The rates at 588 K and the activation energies are also shown in Table 4. The activity of 2 wt% Ru–CsOH/MgO was 20 times as high as that of 2 wt% Ru/MgO. We impregnated MgO with Ru(NO) $(NO_3)_3$ instead of $Ru_3(CO)_{12}$ and added $CsNO_3$ (Cs/Ru = 1/1), then we dried and reduced it at 623 K. This sample had no measurable activity at 623 K. This result is surprising compared to the case of Ru(NO)$(NO_3)_3$/Al_2O_3 (*6*). Because Ru (NO)$(NO_3)_3$ is stored in 3 *N* HNO_3 solution, MgO was impregnated with Ru(NO) $(NO_3)_3$–HNO_3 aqueous solution. Thus, the acid site might be formed on MgO, which may not be neutralized by the alkali addition (Cs/Ru = 1/1) and hydrogen treatment.

Activities of 2 wt% Ru/MgO promoted with various alkali earth metal nitrates are shown as a function of reciprocal temperature in Fig. 4. The extent of the noted promotion effects is inversely related to the electronegativity of the compounds (BaO < SrO < CaO). However, the activities are clearly much lower than that observed after promotion with alkali metal nitrates. Nevertheless, Ru–BaO/MgO is three times as active as Ru/MgO (Table 4), and Ru–CaO/MgO (Table 4) is much more active than Ru/CaO (Table 1). It is interesting to point out that Ba^{2+} was as effective as Cs^+ for Ru/AC (active carbon) (*14*). The reason for this effectiveness is discussed later. Activities at 588 K are also shown in Table 4.

Activities of 2 wt% Ru/MgO with vari-

TABLE 3

Effect of Al_2O_3 Addition to MgO in Ammonia Synthesis under 101 kPa of $N_2 + 3H_2$ over 2 wt% Ru/Al_2O_3–MgO[a]

Al precursor	Mg precursor	Al mol%[b]	Method	Rate (μmol NH_3 h^{-1} g^{-1})		E_a (kcal mol^{-1})
				673 K	623 K	
None	MgO	0	—	379	170	28.5
$Al(NO_3)_3$	$Mg(OH)_2$	10.0	Impregnation	281	—	—
$Al(NO_3)_3$	$Mg(NO_3)_2$	10.0	Urea	226	75	19.2
$Al(NO_3)_3$	$Mg(NO_3)_2$	10.0	NH_4OH	294	97	18.5
$Al(NO_3)_3$	MgO	10.0	NH_4OH	269	84	19.5
$Al(NO_3)_3$	MgO	2.1	Impregnation[c]	285	92	18.9

[a] $Ru_3(CO)_{12}$.

[b] Al/(Al + Mg) was impregnated after supports were calcined in air at 773 K. All catalysts were treated with hydrogen at 673 K for 4 h.

[c] The support was calcined in air at 873 K.

ous lanthanide nitrates are displayed in Fig. 5. They are more active than 2 wt% Ru/MgO, but the promoter effects are not remarkable. Lanthanides have been reported to be as effective as Cs^+ for Ru/Al_2O_3 for reasons discussed elsewhere (*7*).

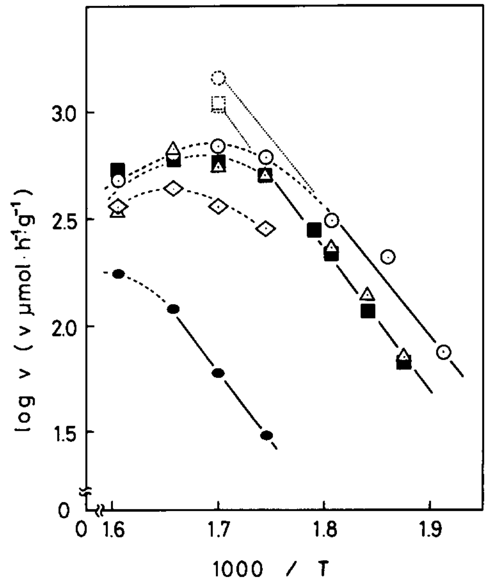

FIG. 3. Arrhenius plot of ammonia synthesis under 80 kPa $N_2 + 3H_2$ over 2 wt% Ru/MgO promoted with various alkali metal nitrates (*M*/Ru = 1/1 mol ratio). (○) Cs^+, (■) Rb^+, (△) K^+, (◇) Na^+, (●) without promoter.

The activities at 588 K are also summarized in Table 4.

Promoter Effect of $Ba(NO_3)_2$ on Ru/MgO

Previous studies disclosed that the decomposition behavior of a promoter nitrate is important in determining the Ru–promoter interaction (*7*, *14*). We studied the effects of $Ba(NO_3)_2$ content and decomposition temperature on Ru/MgO. $Ba(NO_3)_2$ was the most effective promoter precursor among the alkali earth metals. The activities of 2 wt% Ru–BaO/MgO at 588 K are shown as a function of the Ba/Ru mol ratio in Fig. 6. Maximum activity was obtained with Ba/Ru equaling 1/1 (mol ratio) for MgO support with 2 wt% Ru; for active carbon support, the maximum was performed at a Ba/Ru ratio of 20/1 with 2 wt% Ru (*14*).

We measured the activities of 2 wt% Ru–BaO/MgO (Ba/Ru = 1/1) treated in hydrogen at various temperatures. The results are shown in Fig. 7. Activities at 573 K were 224, 180, and 87 μmol h^{-1} g^{-1} for the reduction temperatures of 573, 623, and 673 K, respectively. The high-temperature treatment yields low activity, which is different from the reduction behavior for an alkali metal nitrate (Fig. 7).

TABLE 4

Promoter (M) Effect on 2 wt% Ru/MgO (M/Ru = 1 mol ratio)[a] for NH_3 Synthesis under 80 kPa of N_2 + $3H_2$

Promoter	Rate (μmol NH_3 h^{-1} g^{-1})		E_a (kcal mol^{-1})
	588 K	573 K	
None	60	—	30
Alkali metal			
Na^+	361	—	—
K^+	563 (1059)[b]	—	30
Rb^+	581 (1089)[b]	—	31
Cs^+	690 (1445)[b]	—	27
Alkali earth metal			
Ca^{2+}	135	—	—
Sr^{2+}	113	—	—
Ba^{2+}	213	149	—
Rare earth metal			
La^{3+}	115	57	—
Ce^{3+}	100	85	—
Pr^{3+}	129	69	—
Nd^{3+}	140	57	—
Sm^{3+}	86	49	—
Gd^{3+}	93	57	—
Dy^{3+}	118	73	—

[a] Promoter precursors are nitrates. Samples were reduced at 623 K.

[b] Extrapolated values in parentheses are based on each activation energy. They represent the values expected from the straight line in the lower-temperature region.

$CsNO_3$ Promoter Decomposition on Ru/MgO

Because we found cesium nitrate to be the best promoter for chlorine-free Ru/MgO among 14 promoter compounds, we studied in detail the 2 wt% Ru–CsOH/MgO. We measured hydrogen pressure drop during the pretreatment of 2 wt% Ru–$M$$NO_3$/MgO ($M$/Ru = 1/1; M = Cs, Rb, or K; and weight of 2 wt% Ru/MgO = 1 g). The temperature was raised at a rate of about 6 K/min from 298 to 600 K (50 min), then raised slowly for 1 h up to 623 K, where it was kept for about 4 h. Produced ammonia and water were condensed in a liquid nitrogen trap. The hydrogen pressure drop correlated with temperature is shown in Fig. 8. A previous study has shown that $CsNO_3$ decomposes at approximately 473 to 523 K in the case of a $RuCl_3$–$CsNO_3$ mixture (*2*). Here, the decomposition occurs at a temperature 100 K lower (373 to 423 K). $CsNO_3$ is more active than $RbNO_3$ and KNO_3. In the case of the $RuCl_3$–$CsNO_3$ mixture, $RuCl_3$ must first be reduced to Ru metal, which acts as a catalyst for $CsNO_3$ decomposition. Here, Ru metal clusters have already been formed when $Ru_3(CO)_{12}$/MgO is decomposed at 623 K before adding $CsNO_3$. Such a situation and the fineness of Ru particles may cause this Cl-free Ru/MgO to be active for $CsNO_3$ decomposition at the low temperature. The observed pressure drop (50 Torr) must be adjusted by a pressure increase (dotted line in Fig. 8, 21 Torr) due to the reactor heating 298 to 423 K in order to estimate the real pressure drop (71 Torr) in this apparatus (203 ml volume). This value corresponds to

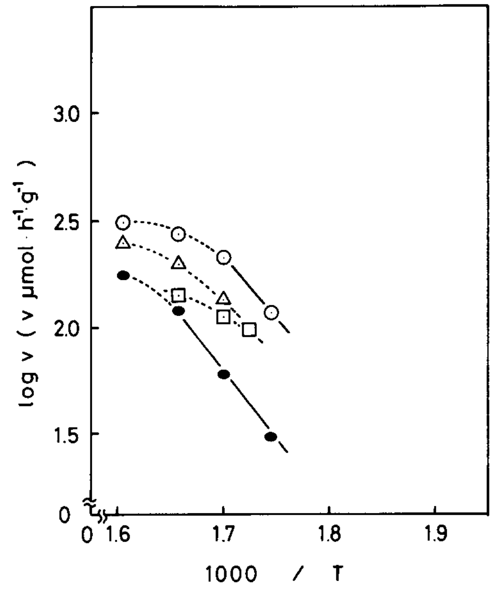

FIG. 4. Arrhenius plot of ammonia synthesis under 80 kPa N_2 + $3H_2$ over 2 wt% Ru/MgO promoted with various alkali earth metal nitrates (*M*/Ru = 1/1 mol ratio). (○) Ba^{2+}, (□) Sr^{2+}, (△) Ca^{2+}, (●) without promoter.

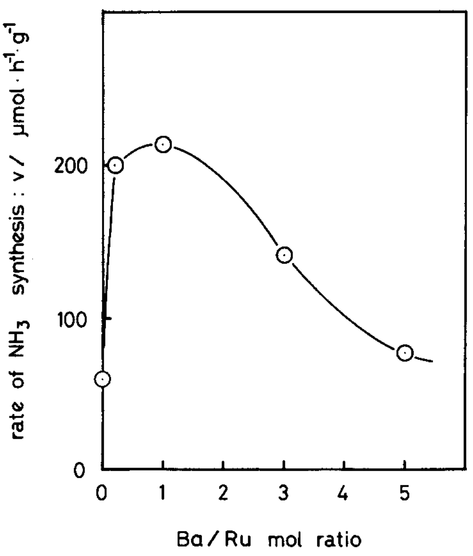

FIG. 6. Rate of ammonia synthesis at 588 K under 80 kPa N_2 + $3H_2$ on 2 wt% Ru–Ba^{2+}/MgO as a function of Ba/Ru mol ratio.

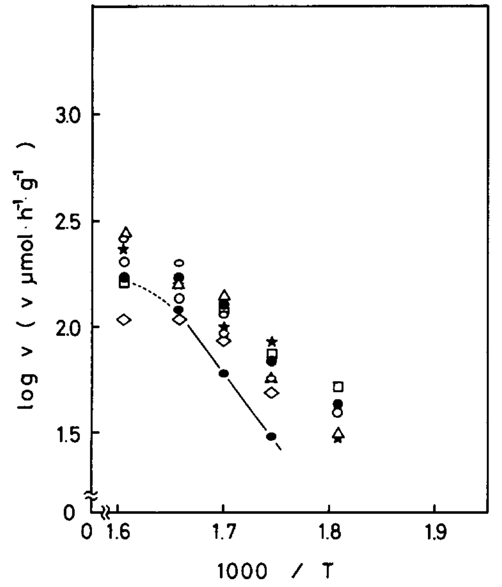

FIG. 5. Arrhenius plot of ammonia synthesis under 80 kPa N_2 + $3H_2$ over 2 wt% Ru/MgO promoted with various rare earth metal nitrates (*M*/Ru = 1 mol ratio). (o) La^{3+}, (★) Ce^{3+}, (●) Pr^{3+}, (△) Nd^{3+}, (◇) Sm^{3+}, (○) Gd^{3+}, (□) Dy^{3+}, (●) without promoter.

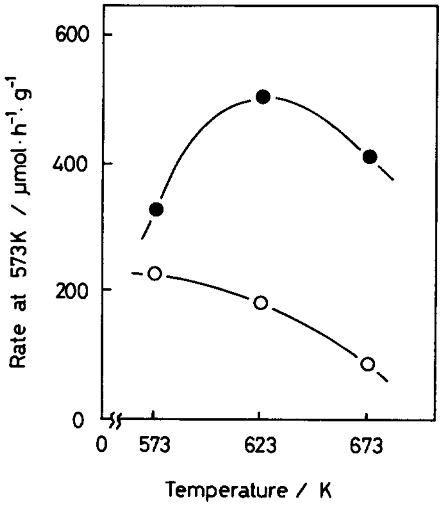

FIG. 7. Rate of ammonia synthesis at 588 K under 101 kPa N_2 + $3H_2$ on 2 wt% Ru–BaO/MgO (N_2 + $3H_2$ = 600 Torr) and 2 wt% Ru–CsOH/MgO correlated with the hydrogen treatment temperature. (●) Cs^+, (○) Ba^{2+}.

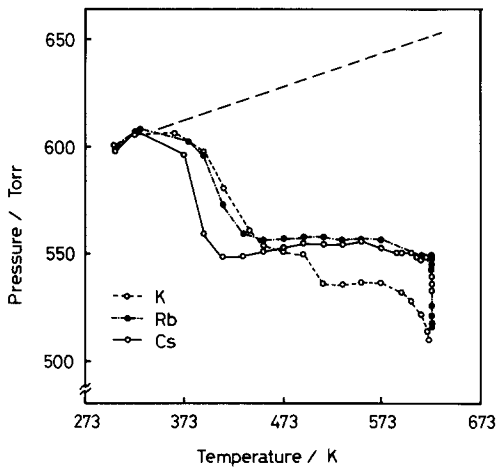

FIG. 8. Change in hydrogen pressure during the hydrogenolysis of alkali metal nitrates over 2 wt% Ru/MgO. Temperature was increased at a rate of 6 K min^{-1} to 600 K (50 min), then increased slowly to 623 K (1 h) where it was kept for 4 h. Produced ammonia and water are condensed in a liquid nitrogen trap. Dotted line indicates the pressure increase due to the heating of the reactor (16 ml).

0.78 mmol consumption of H_2. Because this value is four times the amount of $CsNO_3$ (0.2 mmol), either of the following two reactions probably occur during the pretreatment:

$$2CsNO_3 + 8H_2 \rightarrow Cs_2O + 2NH_3 + 5H_2O \quad (1)$$

$$CsNO_3 + 4H_2 \rightarrow CsOH + NH_3 + 2H_2O. \quad (2)$$

This yields the same conclusion for the decomposition of $CsNO_3$ on Ru catalyst studied previously (2). However, hydrogen consumption also occurs slowly at higher temperatures (523–623 K), perhaps because the surface-reducible species, such as CO_3^{2-}, consumes hydrogen at 523–623 K. During the reduction of $RuCl_3$/MgO, methane formation was initially observed (2). The induction period of ammonia synthesis over Ru/MgO is also thought to be due to CO_2 poisoning.

The effect of the decomposition temperature of $CsNO_3$ on the activity of Ru/MgO is shown in Fig. 7. Although the decomposition of $CsNO_3$ is completed below 573 K, the activity at 573 K decomposition is lower than that at 623 K, possibly because of the CO_2 poisoning described above.

Characterization and Activity of Ru–CsOH/MgO

We measured activities of 2 wt% Ru/MgO with various amounts of $CsNO_3$ by both a flow system and a circulation system. The results are shown as a function of reciprocal temperature in Fig. 9. The apparent activation energies obtained were 29 ± 2 kcal mol^{-1}. Activities at 588 K were correlated with Cs content and compared with the results of 2 wt% Ru–CsOH/Al_2O_3 (Fig. 10). The maximum activity occurred at a Cs/Ru ratio of 1/1 to 2/1. The actual activities must be higher if the Arrhenius plots are extrapolated over the equilibrium limit. We found a small amount of Cs^+ to be quite effective on Ru/MgO, but Ru/Al_2O_3 required a large amount of the element.

We measured the XPS spectra of unreduced 2 wt% Ru/MgO, 623 K-reduced 2

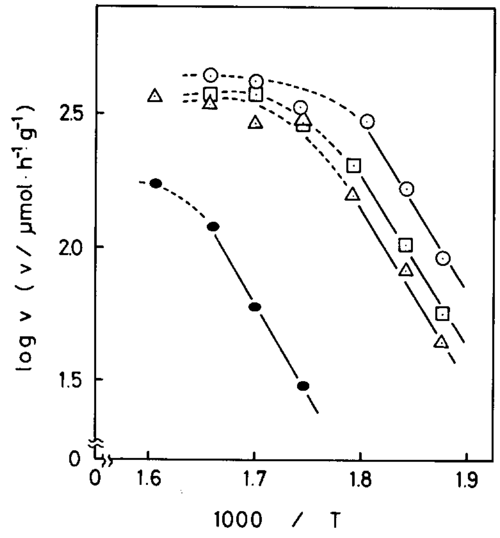

FIG. 9. Arrhenius plot of ammonia synthesis under 80 kPa N_2 + $3H_2$ over 2 wt% Ru–Cs^+/MgO with various Cs/Ru mol ratios. (●) Cs/Ru as 0/1, (△) Cs/Ru as 0.26/1, (○) Cs/Ru as 1/1, (□) Cs/Ru as 4/1.

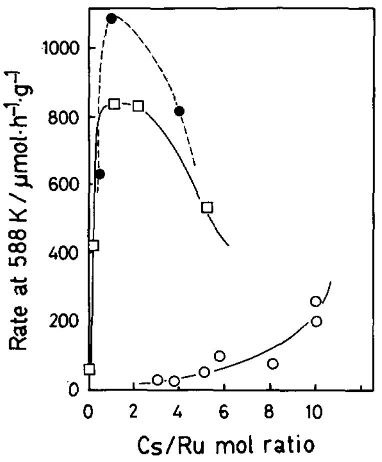

FIG. 10. Rate of ammonia synthesis at 588 K under 101 kPa N_2 + $3H_2$ over 2 wt% Ru–CsOH/MgO (□ and ●) and 2 wt% Ru–CsOH/Al_2O_3 (○) as a function of Cs/Ru mol ratio. The catalysts were reduced with H_2 at 623 K for 4 h. Data with ● are taken under 80 kPa of N_2 + $3H_2$ and are modified to extrapolate the Arrhenius plot (see Table 6).

wt% Ru/MgO, and 5 wt% Ru–CsOH/MgO (Cs/Ru = 1/1). The results are shown in Table 5. A peak shoulder in O 1*s* peak observed for unreduced 2 wt% Ru/MgO sample was attributed to OH (531.7 eV) and disappeared after the reduction. Reduced 2 wt% Ru/MgO and 5 wt% Ru–CsOH/MgO gave only single peaks due to O^{2-} (530.3 ± 0.1 eV for O 1*s*). The binding energy of Ru $3p_{3/2}$ and Ru $3d_{5/2}$ for unreduced Ru/MgO sample was changed from 462.2 and 280.5 eV to 462.1 and 280.1 eV by hydrogen reduction, respectively. The last values show that Ru is reduced to metal. It is interesting to point out that the Ru/MgO sample before reduction (462.2 eV for Ru $3p_{3/2}$) is not completely oxidized, as is the case of Ru/Al_2O_3 (463.4 eV for Ru $3p_{3/2}$) (*6*). MgO seems to prevent the oxidation of Ru in air. Nevertheless, EXAFS data indicate that Ru is situated between a metal and an oxide in Ru/MgO. The binding energy of Cs $3d_{5/2}$ for 5 wt% Ru–CsOH/MgO was 725.1 eV, which suggests that Cs^+ exists as CsOH (725.5 eV) rather than as $CsNO_3$ (726.0 eV).

BET area and hydrogen adsorption were measured for two series of 2 wt% Ru–CsOH/MgO catalysts. The results are shown as a function of Cs/Ru mol ratio in Fig. 11. The MgO sample shown in (a) has a high surface area (90 $m^2 g^{-1}$); that in (b) has a low surface area (36 $m^2 g^{-1}$). The two MgO samples were obtained from the same company, but had different grades. The sample with a high surface area was more frequently used for the

TABLE 5

Binding Energy of XPS Spectra of Ru/MgO Catalysts

	Binding energy (eV)				
	O 1*s*	Mg 2*s*	Ru $3p_{3/2}$	Ru $3d_{5/2}$	Cs $3d_{5/2}$
2 wt% Ru/MgO[a]	530.4	88.1	462.2	280.5	
2 wt% Ru/MgO[b]	530.4	88.0	462.1	280.1	
5 wt% Ru–CsOH/MgO[c]	530.2	87.8	461.4	280.1	725.1
Ru powder			462.0	280.0	
$Mg(OH)_2$	531.7	88.3			
MgO	530.0	87.8			
Cs^+ (*15*)					724.0
CsOH (*16*)	531.7				725.5
$CsNO_3$ (*16*)					726.0

[a] Unreduced.
[b] Reduced in H_2 at 623 K.
[c] Reduction in H_2 at 623 K, Cs/Ru = 1/1 (mol ratio).

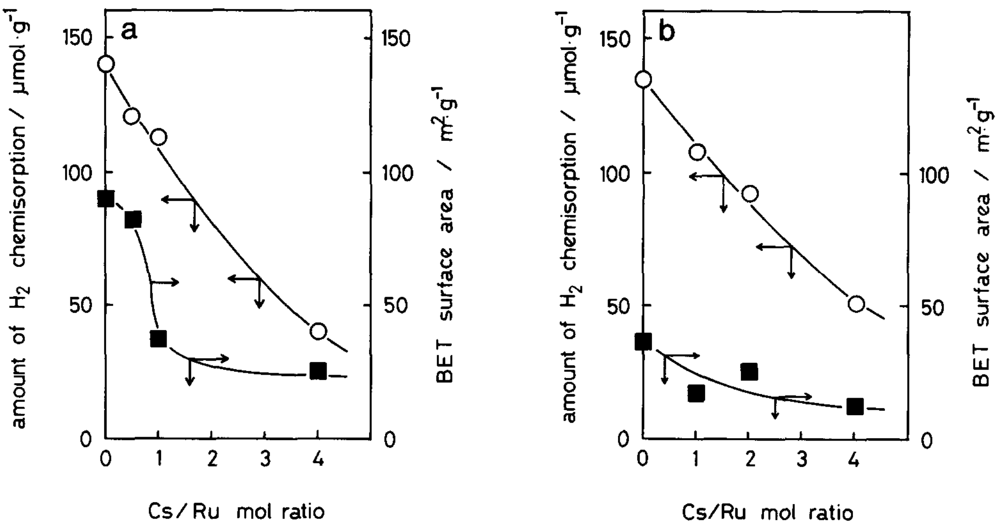

FIG. 11. Hydrogen chemisorption and BET surface area of 2 wt% Ru–CsOH/MgO as a function of Cs/Ru mol ratio. (a) High-surface-area MgO; (b) low-surface-area MgO.

reaction. It is interesting that both samples yielded similar values of high H_2 adsorption, i.e., high Ru dispersion. Ru dispersion and TOF of ammonia synthesis are summarized in Table 6. Because some rate data are saturated by the equilibrium limitation, the real

TABLE 6

Characteristics of Ru/MgO Catalysts

Catalysts		H adsorption (μmol g^{-1})	Rate at 588 K (μmol h^{-1} g^{-1})	TOF × 10^4 at 588 K	H/Ru	P.d.[a] (nm)
Ru/MgO	Ru/wt%					
	1.00	71	40	1.56	0.71	1.9
	1.95	134	60	1.24	0.67	2.0
	5.02	272	181	1.85	0.54	2.5
Ru–CsOH/MgO (Ru/2 wt%)	Cs/Ru (mol ratio)					
	0	134	60	1.24	0.67	2.0
	0.26	121	290 (634)[b]	6.65	0.61	2.2
	1.00	113	418 (1090)[c]	10.26	0.57	2.3
	4.00	40	372 (822)[d]	25.88	0.20	6.4
Ru–CsOH/MgO[e]		208	737 (6180)[f]	9.84	0.42	3.2

[a] Particle diameter calculated from dispersion, (H/Ru).

[b] Calculated as E_a = 29.8 kcal/mol.

[c] Calculated as E_a = 27.4 kcal/mol.

[d] Calculated as E_a = 30.0 kcal/mol.

[e] Ru/5.02 wt%, Cs/Ru = 1/1 mol ratio.

[f] Calculated as E_a = 30.8 kcal/mol.

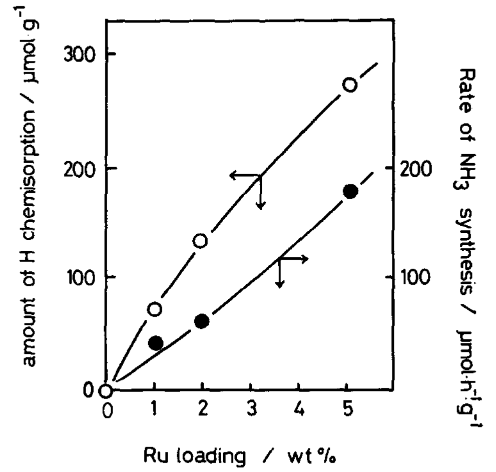

FIG. 12. Rate of ammonia synthesis at 588 K under 80 kPa N_2 + $3H_2$ (●) and hydrogen chemisorption on Ru/MgO (○) as a function of Ru loading.

activity expected from the Arrhenius plot is shown in parentheses.

Design of the Highly Active Catalyst

In order to obtain a highly active catalyst, we increased Ru loading. Figure 12 presents our measurements of the activities of Ru/MgO with various Ru loadings. The activity increases linearly up to 5% of loading. Activation energies were 28 ± 1 kcal/mol for the 1, 2, and 5% Ru/MgO. The high-surface-area MgO was used as a support with 5 wt% Ru loading. We also assessed hydrogen chemisorption (Fig. 12). It should be noted that the high dispersion is maintained even for 5 wt% Ru/MgO. Thus, the $CsNO_3$ was added to this sample. The ammonia synthesis rate was measured and is shown in Fig. 13. As expected, activity was quite high. This is one of the best catalysts for ammonia synthesis under 80 kPa of N_2 + $3H_2$.

DISCUSSION

Ru–Support Interaction

As is summarized in Table 1, the activity of the supported Ru catalyst depends upon the basicity or electronegativity of elements. Roughly speaking, the activity order (MgO > CaO > Al_2O_3 > Nb_2O_5 = TiO_2) is inversely related to the order of electronegativity of the compound: CaO(1.87) < MgO(2.05) < Al_2O_3(2.49) < TiO_2(2.64) < Nb_2O_5(2.80).

Several attempts to increase surface basicity, such as doping MgO with alkali metals ion (Table 2) or mixing MgO with Al_2O_3 (Table 3), did not increase the Ru activity. As evident in the results shown in Tables 1 to 4, the chemical nature of the support was important for the activation of dinitrogen on Ru, although Ru–support interaction is not remarkable when compared with Ru–promoter interaction. This is primarily because the promoter can interact effectively with the Ru metal cluster due to the promoter's activation on the Ru surface.

Importance of Basicity of Promoter for Ammonia Synthesis on Ru/MgO

Because Ru/MgO has no chlorine, the promoter is not a neutralizer of chlorine but

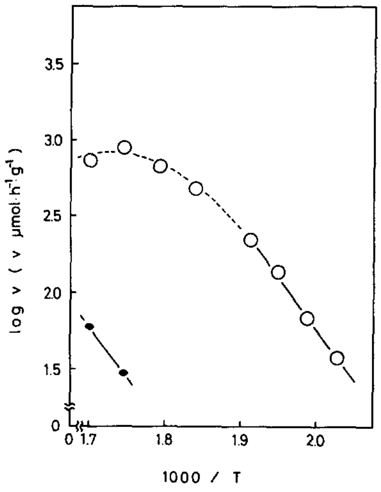

FIG. 13. Arrhenius plot of ammonia synthesis under 80 kPa N_2 + $3H_2$ over the highly active catalyst, 5 wt% Ru-CsOH/MgO (Cs/Ru = 1/1) (○), and over 5 wt% Ru/MgO (●).

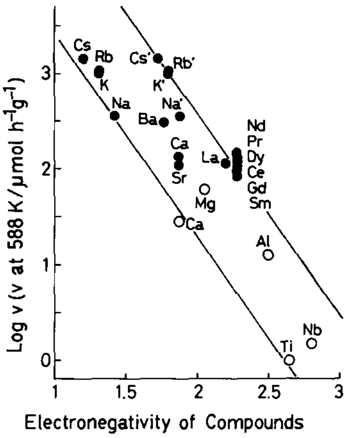

FIG. 14. Logarithms of ammonia synthesis rate at 588 K over Cl-free 2 wt% Ru catalysts correlated with the electronegativity of promoter or support compounds. MgO, CaO, Al_2O_3, TiO_2, and Nb_2O_5 are supports without promoters (○) and others are the promoters (*M*) of 2 wt% Ru/MgO (*M*/Ru = 1/1 mol ratio) catalyst (●). Rate data are taken from Tables 1 and 4. Apparent activation energies for TiO_2 and Nb_2O_5 are assumed to be the same as for Al_2O_3, and the activation energy of CaO is assumed to be the same as for MgO. Plain element name represents oxides of alkali metal (M_2O), alkali earth metal (*M*O), rare earth metal (M_2O_3), Al_2O_3, TiO_2, and Nb_2O_5, whereas the dotted element name indicates alkali metal hydroxides (*M*OH).

rather an electronic modifier of the Ru surface. The effectiveness of the promoter is illustrated in Fig. 14, where the activity at 588 K is displayed as a function of the electronegativity of the promoter compound, which must be related to its surface basicity. An electronegativity of compound is the geometric mean value of Pauling's electronegativities of its elements. Alkali metals have two kinds of values: one is as an oxide and the other is as a hydroxide. The effects of supports and promoters on MgO are shown in the same figure. We can identify the rough trend toward highly active compounds with low electronegativity.

However, we must consider the morphologic aspect when we admit the following: (1) rare earth metal oxides are rather effective considering their high electronegativity values, and (2) the same oxide seems more effective used as a promoter than as a support (CaO). A similar relationship has already been shown for the sample started from $RuCl_3$, but it may contain a Cl ion effect (*3*). Here the role of the promoter is discussed in relation to electron transfer to the Ru surface.

Alkali metal promoter can give electrons to the Ru surface. The electron transfer reaction comprises two steps: the radical process (Eq. (3)) and the second acid–base process (Eq. (4)), in which ·Ru–Ru–Ru· is a metal cluster model:

$$\mathrm{Cs}\cdot + \cdot\mathrm{Ru{-}Ru{-}Ru}\cdot \rightleftarrows (\mathrm{Cs{-}Ru{-}Ru{-}Ru}\cdot) \qquad (3)$$

$$(\mathrm{Cs{-}Ru{-}Ru{-}Ru}\cdot) \rightleftarrows \mathrm{Cs}^+ + (:\mathrm{Ru{-}Ru{-}Ru}\cdot)^-. \qquad (4)$$

Basic oxide or hydroxide may give electrons in an acid–base process (Eqs. (5) and (6)).

$$\mathrm{Cs{-}O{-}H} + \cdot\mathrm{Ru{-}Ru{-}Ru}\cdot \rightleftarrows ({}^{\mathrm{Cs}}_{\mathrm{H}}\!> \mathrm{O}\!: \mathrm{R}\dot{\mathrm{u}}\mathrm{{-}Ru{-}Ru}\cdot) \qquad (5)$$

$$({}^{\mathrm{Cs}}_{\mathrm{H}}\!> \mathrm{O}\!: \dot{\mathrm{R}}\mathrm{u{-}Ru{-}Ru}\cdot) \rightleftarrows \mathrm{Cs}^+ + (\mathrm{H{-}O{-}R}\dot{\mathrm{u}}\mathrm{{-}Ru{-}Ru}\cdot)^-. \qquad (6)$$

Thus, the ability to release electrons to the Ru metal cluster is related to the low electronegativity of metal (such as Cs) to move reaction (4) or (6) to the right-hand side and with the low electronegativities of counter element (such as O or H) to move the electron to the Ru cluster in the anion. If Cs_2O is used instead of CsOH, electron transfer to Ru in the anion $(\mathrm{Cs{-}O{-}Ru{-}Ru{-}Ru}\cdot)^-$ might be more intensive. This is an explanation modified by the classic acid–base concept (*17*). In the case of CO–metal interaction, Blyholder (*18*) suggested the electron donation from the CO(5σ) molecular orbital into the partially unoccupied *d* orbitals of the metal and a concurrent back donation from the *d* orbitals into the CO antibonding

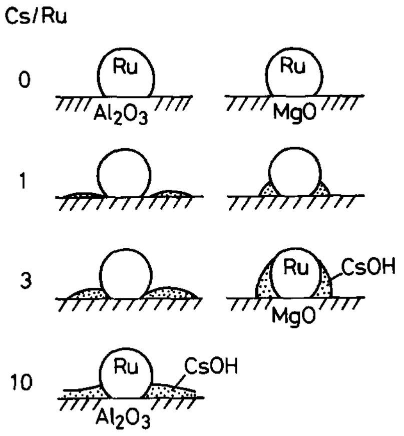

FIG. 15. Schematic picture of CsOH promoter action over Ru/MgO and Ru/Al_2O_3.

$2\pi^*$ orbital. This results in a weakening of the C–O bond, especially in the presence of alkali promoter as evidenced by IR spectroscopy. Because N_2 is isoelectronic to CO, a similar explanation may fit the weakening of the N–N bond (*1–3*).

However, modern surface science stresses the electrostatic field effect explanation, especially for the alkali metal promoter effect (*19, 20*). A strong basic molecule changes the Ru surface's electrostatic field, which might change the molecular orbital level of the adsorbed CO molecule (*19, 20*) or the N_2 molecule (*16*). Both alkali metal and alkali metal hydroxide are believed to affect the electrostatic field of Ru surface in such a way as to activate the N_2 molecule.

The structural factor or surface geometry is important in the case of iron surface (*1*). Although ruthenium is believed to be affected mostly electronically, such a structural factor should be studied in the future. Alkali might affect the surface geometry.

Importance of the Surface Morphology or the Combination of a Support and a Promoter

Promoter action was found to depend on the type of support. A small amount of Ba^{2+} is effective on MgO, but a much greater amount is needed on active carbon (*15*). A small amount of Cs^+ is also quite effective on MgO but Al_2O_3 requires much more (Fig. 10). The hydrogen adsorption on Ru–CsOH/MgO is shown in Fig. 11 and that on Ru–CsOH/Al_2O_3 is shown in Fig. 4 of Ref. (6). Hydrogen adsorption decreases drastically on Ru–CsOH/MgO with an increase of Cs^+, but that is not the case on Ru–CsOH/Al_2O_3. The mechanism of $CsNO_3$ disproportionation is illustrated in Fig. 15. $CsNO_3$ decomposes on the Ru surface and migrates to the support. However, acidic Al_2O_3 may attract Cs^+ more than basic MgO does, leaving less Cs^+ on Ru with Al_2O_3 support. To the contrary, Cs^+ remains more on Ru with MgO support. In the case of Ru–CsOH/MgO, two basic compounds, support (MgO) and promoter (CsOH), can interact well with Ru; in the case of Ru–CsOH/Al_2O_3, some of the CsOH interacts with Ru and most of it interacts with Al_2O_3.

Comparison of the Activity of Ru–CsOH/MgO with Other Catalysts

Figure 16 displays the relative activities of several catalysts. Ru–CsOH/MgO (5 wt%; Cs/Ru = 1/1) was proved to be much more

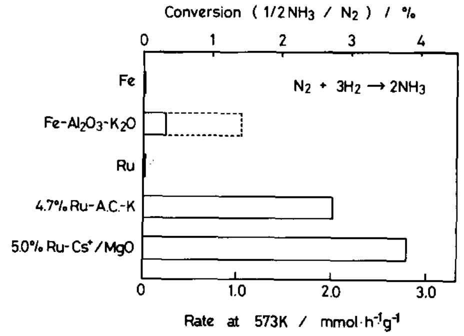

FIG. 16. Comparison of the highly active catalysts, rate of ammonia synthesis at 573 K under 80 kPa $N_2 + 3H_2$. The closed square for Fe–Al_2O_3–K_2O is the data from Ref. (*21*), and the dotted square is the estimated data from Ref. (*8*). Conversion is calculated assuming that 60 ml (NTP) of gas ($N_2 + 3H_2$) passes over 1 g of catalyst per minute.

active than the doubly promoted catalyst and to be as active as 4.7% Ru–K/AC (*1*) or Raney Ru–$CsNO_3$ (*16*), although the last two catalysts were sensitive to air. They are deactivated irreversibly to form Ru–K^+/AC and Raney Ru–CsOH, whereas Ru–CsOH/MgO is only poisoned reversibly (*2*, *3*). Thus, the Ru–CsOH/MgO catalyst can be used practically, if any low-pressure process is expected (*22*).

CONCLUSIONS

Cl-free Ru catalysts were prepared from $Ru_3(CO)_{12}$ for ammonia synthesis. MgO was found to be the best support among several oxides under low-pressure conditions. Modification of MgO to improve the support effect was not successful. Among 14 kinds of metal nitrates, $CsNO_3$ was found to be the most effective for Ru/MgO. Among the alkali earth metal oxides, $Ba(NO_3)_2$ was also effective. The role of the promoter was clarified using Cl-free Ru/MgO. $CsNO_3$ decomposition over Ru/MgO was studied. Hydrogen consumption results disclosed that $CsNO_3$ was easily decomposed to Cs_2O or CsOH with the aid of the Ru surface. A morphologic model between CsOH and Ru was proposed. The activity of 5% Ru–CsOH/MgO was as great as that of 5% Ru–K/AC or Raney Ru–$CsNO_3$. Although the former is not irreversibly poisoned by oxygen-containing compounds, the latter two are. The catalyst we prepared is quite active and stable under atmospheric pressure. Thus, further study should be made into appropriate industrial applications.

ACKNOWLEDGMENTS

The authors acknowledge Dr. K. Asakura of the University of Tokyo and Professor Emeritus T. Onishi of the Tokyo Institute of Technology for the discussions.

REFERENCES

1. Ozaki, A., and Aika, K., *in* "Catalysis-Science and Technology" (J. R. Anderson and M. Boudart, Eds.), Vol. 1, p. 87. Springer-Verlag, New York, 1981.

2. Aika, K., Shimazaki, K., Hattori, Y., Ohya, A., Oshima, S., Shirota, K., and Ozaki, A., *J. Catal.* **92,** 296 (1985).

3. Aika, K., Ohya, A., Ozaki, A., Inoue, Y., and Yasumori, I., *J. Catal.* **92,** 305 (1985).

4. Aika, K., Kumasaka, M., Oma, T., Kato, O., Matsuda, H., Watanabe, N., Yamazaki, K., Ozaki, A., and Onishi, T., *Appl. Catal.* **28,** 57 (1986).

5. Murata, S., and Aika, K., *Appl. Catal.*, **82,** 1 (1992).

6. Murata, S., and Aika, K., *J. Catal.*, **136,** 110 (1992).

7. Murata, S., and Aika, K., *J. Catal.*, **136,** 118 (1992).

8. Amarigrio, H., and Rambeau, G., *in* "Proceedings, 6th International Congress on Catalysis, London, 1976" (G. C. Bond, P. B. Wells, and F. C. Tompkins, Eds.), p. 1113. The Chemical Society, London, 1977.

9. Asakura, K., Yamada, M., Iwasawa, Y., and Kuroda, H., *Chem. Lett.* 511 (1985).

10. Zecchina, A., Guglielminotti, E., Bossi, A., and Camia, M., *J. Catal.* **74,** 225 (1982).

11. Iwamatsu, E., Moriyama, T., Takasaki, N., and Aika, K., *J. Catal.* **113,** 25 (1988).

12. Matsuda, T., Minami, Z., Shibata, Y., Nagano, S., Miura, H., and Sugiyama, K., *J. Chem. Soc. Faraday Trans. 1* **82,** 1357 (1986).

13. Tanabe, K., Hattori, H., and Yamaguchi, T., *in* "Kagaku Sosetsu, No. 34, Catalysis Design," p. 82. Chemical Society of Japan, Tokyo, 1982.

14. Aika, K., Kawahara, T., Murata, S., and Onishi, T., *Bull. Chem. Soc. Jpn.* **63,** 1221 (1990).

15. Wagner, C. D., Riggs, W. M., Davis, L. E., Moulder, J. F., and Muilenberg, G. E., Eds., "Handbook of X-ray Photoelectron Spectroscopy." Perkin–Elmer Co. Physical Electronics Division, 1978.

16. Hikita, T., Aika, K., and Onishi, T., *Catal. Lett.* **4,** 157 (1990); Hikita, T., Kadowaki, Y., and Aika, K., *J. Phys. Chem.* **95,** 9396 (1991).

17. Vanderwerf, C. A., "Acids, Bases and the Chemistry of the Covalent Bond." Reinhold, New York, 1961.

18. Blyholder, G., *J. Phys. Chem.* **68,** 2772 (1964).

19. Norskov, J. K., Holloway, S., and Lang, N. D., *Surf. Sci.* **137,** 65 (1984).

20. Shyu, J. Z., Goodwin, J. G., Jr., and Hercules, D. M., *J. Phys. Chem.* **89,** 4983 (1985).

21. Ozaki, A., Aika, K., and Morikawa, Y., *in* "Proceedings, 5th International Congress on Catalysis, Palm Beach, 1972" (J. W. Hightower, Ed.), p. 1251. North-Holland, Amsterdam, 1973.

22. Report article in *Appl. Catal.* **67,** N18 (1991).